

Pulse Shape Discrimination in JSNS²

T. Dodo,¹ M. K. Cheoun,² J. H. Choi,³ J. Y. Choi,⁴ J. Goh,⁵ K. Haga,⁶ M. Harada,⁶ S. Hasegawa,^{7,6} W. Hwang,⁵ T. Iida,⁸ H. I. Jang,⁴ J. S. Jang,⁹ K. K. Joo,¹⁰ D. E. Jung,¹¹ S. K. Kang,¹² Y. Kasugai,⁶ T. Kawasaki,¹³ E. J. Kim,¹⁴ J. Y. Kim,¹⁰ S. B. Kim,¹⁵ W. Kim,¹⁶ H. Kinoshita,⁶ T. Konno,¹³ D. H. Lee,¹⁷ I. T. Lim,¹⁰ C. Little,¹⁸ E. Marzec,¹⁸ T. Maruyama,¹⁷ S. Masuda,⁶ S. Meigo,⁶ D. H. Moon,¹⁰ T. Nakano,¹⁹ M. Niiyama,²⁰ K. Nishikawa,¹⁷ M. Y. Pac,³ H. W. Park,¹⁰ J. S. Park,¹⁶ R. G. Park,¹⁰ S. J. M. Peeters,²¹ C. Rott,²² K. Sakai,⁶ S. Sakamoto,⁶ T. Shima,¹⁹ C. D. Shin,^{17,*} J. Spitz,¹⁸ F. Suekane,¹ Y. Sugaya,¹⁹ K. Suzuya,⁶ Y. Takeuchi,⁸ Y. Yamaguchi,⁶ M. Yeh,²³ I. S. Yeoo,³ C. Yoo,⁵ and I. Yu¹¹

(JSNS² Collaboration)

¹Research Center for Neutrino Science, Tohoku University,
6-3 Azaaoba, Aramaki, Aoba-ku, Sendai 980-8578, Japan

²Department of Physics, Soongsil University, 369 Sangdo-ro, Dongjak-gu, Seoul, 06978, Korea

³Laboratory for High Energy Physics, Dongshin University,
67, Dongshindaegil, Naju-si, Jeollanam-do, 58245, Korea

⁴Department of Fire Safety, Seoyeong University, 1 Seogang-ro, Buk-gu, Gwangju, 61268, Korea

⁵Department of Physics, Kyung Hee University, 26,
Kyunghedae-ro, Dongdaemun-gu, Seoul 02447, Korea

⁶J-PARC Center, JAEA, 2-4 Shirakata, Tokai-mura, Naka-gun, Ibaraki 319-1195, Japan

⁷Advanced Science Research Center, JAEA, 2-4 Shirakata, Tokai-mura, Naka-gun, Ibaraki 319-1195, Japan

⁸Faculty of Pure and Applied Sciences, University of Tsukuba,
Tennodai 1-1-1, Tsukuba, Ibaraki, 305-8571, Japan

⁹GIST College, Gwangju Institute of Science and Technology,
123 Cheomdangwagi-ro, Buk-gu, Gwangju, 61005, Korea

¹⁰Department of Physics, Chonnam National University,
77, Yongbong-ro, Buk-gu, Gwangju, 61186, Korea

¹¹Department of Physics, Sungkyunkwan University, 2066,
Seobu-ro, Jangan-gu, Suwon-si, Gyeonggi-do, 16419, Korea

¹²School of Liberal Arts, Seoul National University of Science and Technology,
232 Gongneung-ro, Nowon-gu, Seoul, 139-743, Korea

¹³Department of Physics, Kitasato University, 1 Chome-15-1 Kitazato,
Minami Ward, Sagami-hara, Kanagawa, 252-0329, Japan

¹⁴Division of Science Education, Chonbuk National University,
567 Baekje-daero, Deokjin-gu, Jeonju-si, Jeollabuk-do, 54896, Korea

¹⁵School of Physics, Sun Yat-sen (Zhongshan) University, Haizhu District, Guangzhou, 510275, China

¹⁶Department of Physics, Kyungpook National University, 80 Daehak-ro, Buk-gu, Daegu, 41566, Korea

¹⁷High Energy Accelerator Research Organization (KEK), 1-1 Oho, Tsukuba, Ibaraki, 305-0801, Japan

¹⁸University of Michigan, 500 S. State Street, Ann Arbor, MI 48109, U.S.A.

¹⁹Research Center for Nuclear Physics, Osaka University,
10-1 Mihogaoka, Ibaraki, Osaka, 567-0047, Japan

²⁰Department of Physics, Kyoto Sangyo University,
Motoyama, Kamigamo, Kita-Ku, Kyoto-City, 603-8555, Japan

²¹Department of Physics and Astronomy, University of Sussex, Falmer, Brighton, BN1 9RH, U.K.

²²Department of Physics and Astronomy, University of Utah,
201 Presidents' Cir, Salt Lake City, UT 84112, U.S.A

²³Brookhaven National Laboratory, Upton, NY 11973-5000, U.S.A.

(Dated: April 8, 2024)

JSNS² (J-PARC Sterile Neutrino Search at J-PARC Spallation Neutron Source) is an experiment that is searching for sterile neutrinos via the observation of $\bar{\nu}_\mu \rightarrow \bar{\nu}_e$ appearance oscillations using neutrinos with muon decay-at-rest. For this search, rejecting cosmic-ray-induced neutron events by Pulse Shape Discrimination (PSD) is essential because the JSNS² detector is located above ground, on the third floor of the building. We have achieved 95% rejection of neutron events while keeping 90% of signal, electron-like events using a data driven likelihood method.

I. INTRODUCTION

The existence of sterile neutrinos has been an important issue in the field of neutrino physics for over 20 years. The experimental results from [1–4] could be interpreted

* cdshin@post.kek.jp

as indications of the existence of sterile neutrinos with mass-squared differences of around 1 eV^2 .

The JSNS² experiment, proposed in 2013 [5], searches for short-baseline neutrino oscillations at the Material and Life science experimental Facility (MLF) in J-PARC. The facility provides an intense and high-quality neutrino source with $1.8 \times 10^{14} \nu/\text{year}/\text{cm}^2$ from muon decay-at-rest (μDAR). These neutrinos are produced by impinging 1 MW 3 GeV protons from a rapid cycling synchrotron on a mercury target with 25 Hz repetition in the MLF. The experiment uses a Gadolinium (Gd) loaded liquid scintillator (Gd-LS) detector with 0.1 % Gd concentration placed at 24 m from the target. In addition, diisopropylnaphthalene (DIN, $\text{C}_{16}\text{H}_{20}$) was dissolved into the Gd-LS by 8-10% concentration in volume from 2021.

The JSNS² experiment aims to directly test the LSND observation [1] using improvements on the experimental technique. Observing $\bar{\nu}_\mu \rightarrow \bar{\nu}_e$ oscillation using a μDAR neutrino source via inverse beta decay (IBD) reaction, $\bar{\nu}_e + p \rightarrow e^+ + n$, is the same experimental principle used by LSND experiment [1]. On the other hand, there are several improvements offered by the JSNS² experiment. The main improvements come from using a beam with a low duty factor and a Gd-loaded liquid scintillator, which reduces the accidental background significantly [6].

There are also a number of correlated backgrounds to the IBD signal, characterized by time-coincident prompt and delayed events. The most concerning ones are cosmic-induced neutrons whose prompt signal is made by a recoil proton and a delayed signal from the neutron capture on Gd after thermalization. The first data of JSNS² taken in the commissioning phase in 2020 proves this facts [7]. Therefore, approximately 99% of this neutron background should be rejected by Pulse Shape Discrimination (PSD) using the waveform shape difference between the prompt signal of IBD and neutron events. The JSNS² experiment PSD technique, based on a data driven likelihood method, will be described in this manuscript.

II. JSNS² DETECTOR

The JSNS² detector is described elsewhere [8]. However, in this section, we discuss the most relevant points regarding PSD.

The JSNS² experiment features a cylindrical liquid scintillator detector with 4.6 m diameter and 3.5 m height placed at a distance of 24 m from the mercury target of the MLF. It consists of 17 tonnes of Gd-LS contained in an acrylic vessel, and 33 tonnes unloaded liquid scintillator (LS) in a layer between the acrylic vessel and a stainless steel tank. The LS and the Gd-LS consist of LAB (linear alkyl benzene) as the base solvent, 3 g/L PPO (2,5-diphenyloxazole) as the fluor, and 15 mg/L bis-MSB (1,4-bis(2-methylstyryl) benzene) as the wavelength shifter. The DIN was dissolved into the Gd-LS in the acrylic vessel which has dimensions of 3.2 m of diameter

and 2.5 m of height in order to enhance the PSD capability. DIN is commercially available and widely used as a base solvent of organic liquid scintillator. Several neutrino experiments using a liquid scintillator detector have adopted it and achieved strong PSD capability [9, 10]. Approximately 8% by volume of DIN was dissolved into the Gd-LS at the beginning of the first physics run from January 2021. Nitrogen purging was performed before data taking and nitrogen gas is flowed into the gas phase of the detector to avoid oxygen contamination from outside. Starting from the physics run in 2022, the concentration of DIN was increased from 8% to 10%.

The LS volume is separated into two independent layers by an optical separator that forms two subvolumes in the one detector. The region inside the optical separator, called the “inner detector”, consists of the entire volume of the Gd-LS and ~ 25 cm thick LS layer. Scintillation light from the inner detector is observed by 96 Hamamatsu R7081 photomultiplier tubes (PMTs) each with a 10-inch diameter. The outer layer, called the “veto layer”, is used to detect cosmic-ray induced particles coming into the detector. A total of 24 10-inch PMTs are set in the veto layer whose inner surfaces are fully covered with reflection sheets in order to improve the collection efficiency of the scintillation light.

PMT signal waveforms from both the inner detector and the veto layer are digitized and recorded at a 500 MHz sampling rate by 8-bit flash analog-to-digital converters (FADCs) [11]. A trigger, called the “self trigger”, uses an analog sum of the PMT signals from the inner detector. The trigger threshold is set such that the detection efficiency is approximately 100% above 7 MeV. The FADCs record 496 ns wide waveforms during the data taking using the self trigger. We utilized the self trigger in order to obtain cosmogenic events, and when taking calibration data using a 252-Californium (^{252}Cf) neutron source. The self-trigger is used for the PSD performance study described in this manuscript.

III. DATASET AND EVENT SELECTION

The analysis uses 6 days of data which were taken at the beginning of 2021. Before going into the details of the PSD technique, the event selections of the cosmogenic Michel electrons (ME) and fast neutrons (FN) are described below. These control samples are used to make probability density functions (PDFs) of the likelihood and to evaluate the PSD capabilities which will be described later. The selection criteria for those samples are shown in Table I. In addition to the energy and timing selections, a spatial correlation between prompt and delayed signal (ME: less than 1300 mm, and FN: less than 600 mm) is adopted. Also, the goodness of fit of the energy and vertex reconstruction in the events is used to improve the purity of the control sample; events with goodness variable > 500 are rejected. To reject cosmic muons for ME delayed and FN samples, we require that

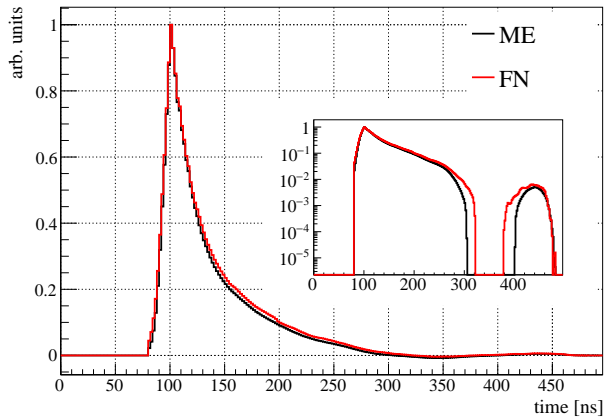


FIG. 1. The typical averaged PMT waveforms of cosmogenic Michel electrons (black) and neutron (red) events.

the top 12 and bottom 12 veto PMTs have less than 100 p.e.. The fiducial volume is defined with $R < 140$ cm and $|z| < 100$ cm region to avoid external backgrounds. Note that origin of the coordinate system is the center of the detector, and R is defined as $R = \sqrt{x^2 + y^2}$. The event reconstruction in JSNS² is described in [12]. With these selections, 387713 ME and 21623 FN events are available for the PSD evaluation and 243310 ME and 15160 FN events are used to make PDFs in this manuscript. Note that the ME sample contains both electrons and positrons and the relevant energy region is identical to the IBD sample.

IV. PRINCIPLE OF PSD

In this section, the principle of the PSD technique is described. The scintillation light created from particle with large local energy loss (dE/dx) creates larger timing tails than those from minimum ionizing particles. Fig. 1 shows the typical averaged PMT waveforms of cosmogenic Michel electrons (black) and neutron events (red), which are observed by the JSNS² detector. The selection criteria will be described later. As shown in this Fig. 1, the waveforms created by the recoiled protons of neutrons have larger tails than that of Michel electrons. PSD will use this difference.

A. Probability Density Function (PDF)

For making the likelihoods for PSD, probability density functions (PDFs) utilizing the pulse height of each FADC bin are created. As shown in Fig. 1, waveforms are recorded every 2 ns, thus the peak normalized pulse height of each 2 ns slice is used to create the PDFs. In the tails, the pulse heights made from ME are distinct from FN events; this difference is utilized for PSD. Each

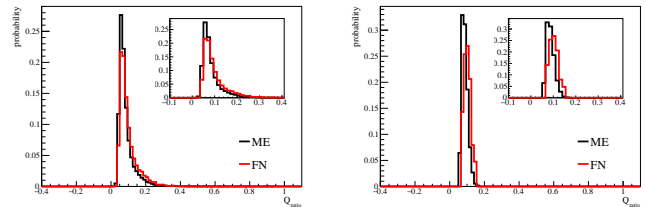


FIG. 2. Typical PDFs of one PMT with around 200 ns of waveforms. Left: a low charge case. Right: a large charge case.

PMT has its own waveform characteristics depending on the received charge but also the power to discriminate the ME and FN alone, therefore the charge dependent PDFs are made for each PMT separately. Note that the large PMT charge creates small fluctuations on the shape of the waveforms. Figure 2 shows a typical PDF of one PMT using around 200 ns of the waveform. Left shows the low charge ($20 < Q < 40$ p.e.) and right shows the high charge ($200 < Q < 220$ p.e.) cases, respectively. Only data are used to make the PDFs.

The waveforms before the real signal, i.e.: before around 80 ns in Fig. 1, is unused for the PSD algorithm. The low charge ($Q < 20$ p.e.) or high charge ($Q > 500$ p.e.) PMTs are also neglected in order to avoid unstable waveforms.

B. Evaluation

The likelihood score is calculated with the following equation:

$$\mathcal{L} = \prod_{i=0}^{95} \prod_{j=40}^{247} [P_{ij}(PH)] \quad , \quad (1)$$

where i is the PMT number of the JSNS² inner detector, which consists of 96 PMTs, j is the index of the FADC time bin (0-248 bins in the self-trigger) such as shown in Fig. 1, and PH is the peak normalized pulse height in j -th bin. $P_j(PH)$ is calculated from the PDFs shown in Fig. 2.

There are two PDFs for the ME and FN, thus the likelihood ratio is calculated with the PDFs as follows:

$$\mathcal{L}_{\mathcal{R}} = \frac{\mathcal{L}^{\mathcal{ME}}}{\mathcal{L}^{\mathcal{FN}}} = \prod_{i=0}^{95} \prod_{j=40}^{247} \frac{[P_{ij}^{\mathcal{ME}}(PH)]}{[P_{ij}^{\mathcal{FN}}(PH)]} \quad (2)$$

For the convenience of the calculation, the log-likelihood is used. Equation 2 is transformed to

$$\begin{aligned} \ln(\mathcal{L}_{\mathcal{R}}) &= \ln(\mathcal{L}^{\mathcal{ME}}) - \ln(\mathcal{L}^{\mathcal{FN}}) \\ &= \sum_{i=0}^{95} \sum_{j=40}^{247} (\ln(P_{ij}^{\mathcal{ME}}(PH)) - \ln(P_{ij}^{\mathcal{FN}}(PH))) \end{aligned}$$

TABLE I. The selection criteria for control samples. Cosmogenic Michel electrons (ME) delayed signal and neutron (FN) prompt signals are used as control samples.

	Energy (ME)	timing (ME)	Energy (FN)	timing (FN)	spatial corr. (Δ_{VTX})	fit goodness
Prompt	10 - 800 MeV		20 - 60 MeV		130 cm (ME)	
Delayed	20 - 60 MeV	$2 < \Delta t < 10\mu s$	7 - 12 MeV	$2 < \Delta t < 100\mu s$	60 cm (FN)	< 500

This log-likelihood ratio provides a positive score for events which are more electron like, while events with negative scores are more neutron like.

V. PSD PERFORMANCE

In this section, the performance of the JSNS² PSD is described. To avoid bias, the control sample for making the PDFs and evaluating performance are separated and different dataset are used. Fig. 3 shows the PSD score distributions. As mentioned, events with positive score are electron like events, while those with negative score are neutron like events. The black corresponds to ME and the red to the FN control samples using the event selection shown in Table I.

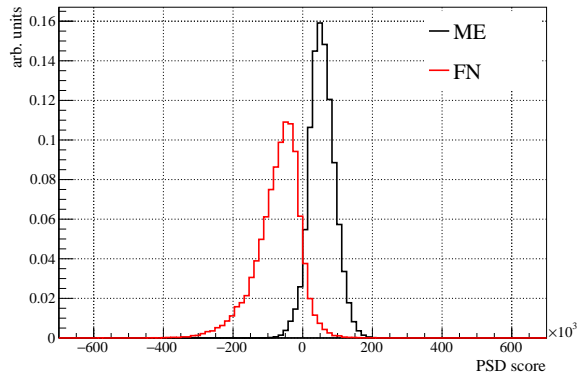


FIG. 3. PSD score distributions on the log-likelihood ratio.

The relationship between the FN rejection factor and ME efficiency is seen in Fig. 4. Requiring $95.32 \pm 0.15\%$ of FN rejection, the ME efficiency is about $89.30 \pm 2.78\%$, with the uncertainties including systematics.

VI. CONCLUSION

JSNS² has developed a log-likelihood based PSD to differentiate neutron background from signal electron-like events. Due to the DIN dissolved liquid scintillator and sophisticated likelihood techniques, described in this paper, we achieved $95.32 \pm 0.15\%$ neutron event rejection while keeping the signal like electron efficiency of $89.30 \pm 2.78\%$, noting that the rejection factor can be increased depending on the analyses. JSNS² will adopt this

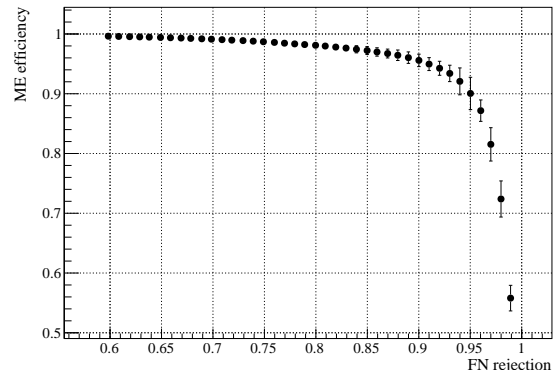


FIG. 4. The relationship between the FN rejection factor (horizontal) and ME efficiency (vertical).

PSD technique for in searching for short-baseline oscillations involving a sterile neutrino.

ACKNOWLEDGMENTS

We deeply thank the J-PARC staff for their supports, especially for the MLF and accelerator groups to provide the good opportunities of this experiment. We acknowledge the support of the Ministry of Education, Culture, ports, Science, and Technology (MEXT) and the JSPS grants-in-aid: 16H06344, 16H03967 23K13133 and 20H05624, Japan. This work is also supported by the National Research Foundation of Korea (NRF): 2016R1A5A1004684, 17K1A3A7A09015973, 2017K1A3A7A09016426, 2019R1A2C3004955, 2016R1D1A3B02010606, 2017R1A2B4011200, 2018R1D1A1B07050425, 2020K1A3A7A09080133, 2020K1A3A7A09080114, 2020R1I1A3066835, 2021R1A2C1013661, 2022R1A5A1030700 and RS-2023-00212787. Our work has also been supported by a fund from the BK21 of the NRF. The University of Michigan gratefully acknowledges the support of the Heising-Simons Foundation. This work conducted at Brookhaven National Laboratory was supported by the U.S. Department of Energy under Contract DE-AC02-98CH10886. The work of the University of Sussex is supported by the Royal Society grant no. IESnR3n170385. We also thank the Daya Bay Collaboration for providing the Gd-LS, the RENO collaboration for providing the LS and PMTs, CIEMAT for providing the splitters,

Drexel University for providing the FEE circuits and Tokyo Inst. Tech for providing FADC boards

- [1] C. Athanassopoulos *et al.* (LSND collaboration), Phys. Rev. Lett. **77**, 3082 (1996).
- [2] V. V. Barinov *et al.* (BEST collaboration), Phys. Rev. C **105**, 065502 (2022).
- [3] A. A. A. Arevalo *et al.* (MiniBooNE collaboration), Phys. Rev. Lett. **120**, 141802 (2018).
- [4] G. Mention, M. Fechner, T. Lasserre, T. A. Mueller, D. Lhuillier, M. Cribier, and A. Letourneau, Phys. Rev. D **83**, 073006 (2011).
- [5] M. Harada *et al.* (JSNS² collaboration), (2013), physics.ins-det/1310.1437.
- [6] S. Ajimura *et al.* (JSNS² collaboration), (2017), physics.ins-det/1705.08629.
- [7] Y. Hino *et al.* (JSNS² collaboration), Euro. Phys. Joun. C **82**, 331 (2022).
- [8] S. Ajimura *et al.* (JSNS² collaboration), Nucl. Inst. and Meth. A **1014**, 165742 (2021).
- [9] B. R. Kim *et al.* (NEOS collaboration), J. Radioanal. Nucl. Chem. **310**, 311 (2016).
- [10] J. Ashenfelter *et al.*, Journal of Instrumentation **14**, No.3 P03026 (2019).
- [11] J. S. Park *et al.*, Journal of Instrumentation **15**, No.9 T09002 (2020).
- [12] J. R. Jordan's PhD thesis, <https://dx.doi.org/10.7302/6288>.